

CERN-TH/97-284

Parton Distributions from Photoproduction in Polarized ep Scattering at HERA

Werner Vogelsang*

Theory Division, CERN, CH-1211 Geneva, Switzerland

Abstract

We study photoproduction of jets and single-inclusive hadrons in a polarized ep collider mode of HERA at $\sqrt{s} \approx 300$ GeV, examining the sensitivity of the cross sections and their asymmetries to the proton's polarized gluon distribution and to the completely unknown parton distributions of polarized photons. We also present for the first time the NLO corrections to the direct part of polarized single-inclusive hadron photoproduction.

1 Introduction

Among the various conceivable options for future HERA upgrades is the idea to longitudinally polarize its proton beam [1] which, when combined with the already operative longitudinally polarized electron (positron) beam, results in a polarized version of the usual HERA collider with $\sqrt{s} \approx 300$ GeV. A typical conservative value for the integrated luminosity in this case should be 100 pb^{-1} .

HERA has already been very successful in pinning down the proton's unpolarized gluon distribution $g(x, Q^2)$. Several processes have been studied which have contributions from $g(x, Q^2)$ already in the lowest order, such as (di)jet, inclusive hadron, and heavy flavour production. Since events at HERA are concentrated in the region $Q^2 \rightarrow 0$, the processes have first and most accurately been studied in photoproduction [2-7]. As is well-known, in this case the (quasi-real) photon will not only interact in a direct ('point-like') way, but can also be resolved into its hadronic structure. HERA photoproduction experiments like [2-7] have not merely established evidence for the existence of such a resolved contribution, but have also been precise enough to improve our knowledge about the parton distributions, f^γ , of the photon.

Given the success of such unpolarized photoproduction experiments at HERA, it seems most promising [8] to closely examine the same processes for the situation with longitudinally polarized beams with regard to their sensitivity to the proton's polarized gluon distribution Δg , which is still one of the most interesting, but least known, quantities in 'spin-physics'. Recent next-to-leading (NLO) studies of polarized DIS [9-12] show that the x -shape of Δg seems to be hardly constrained at all by the present DIS data, even though a tendency towards a sizeable positive *total* gluon polarization, $\int_0^1 \Delta g(x, Q^2 = 4 \text{ GeV}^2) dx \gtrsim 1$, was found [9, 13, 10]. Furthermore, polarized photoproduction experiments may in principle allow to not only determine the parton, in particular gluon, content of the polarized *proton*, but also that of the longitudinally polarized *photon* which is completely unknown so far. Since a measurement of, e.g., the photon's spin-dependent structure function g_1^γ in polarized e^+e^- collisions is not planned in the near future, polarized HERA could play a unique role here, even if it should only succeed in establishing the very *existence* of a resolved contribution to polarized photon-proton reactions.

*Invited talk presented at the workshop 'Deep Inelastic Scattering off Polarized Targets: Theory Meets Experiment', Zeuthen, Germany, September 1-5, 1997

Our contribution is organized as follows: In the next section we collect the necessary ingredients for our calculations. In sec. 3 we will discuss at leading order (LO) the most promising photoproduction reactions, namely (di)jet and single-inclusive hadron production. Part of this section is taken from [8]. Sec. 4 will then present for the first time the NLO corrections to the direct part of the latter process. More details on the results presented in sec. 4 will be published in [14].

2 Spin-dependent Parton Distributions of the Proton and the Photon

Our main calculations will be performed at LO, as the NLO corrections to the spin-dependent parts of the photoproduction processes we are interested in are usually not yet available. This implies use of LO parton distributions, which have been provided in the analyses [9, 10] of recent polarized DIS data. Both papers give various LO sets which mainly differ in the x -shape of the polarized gluon distribution. We will choose the LO ‘valence’ set of the ‘radiative parton model analysis’ [9], which corresponds to the best-fit result of that paper, along with two other sets of [9] which are based on either assuming $\Delta g(x, \mu^2) = g(x, \mu^2)$ or $\Delta g(x, \mu^2) = 0$ at the low input scale μ of [9], where $g(x, \mu^2)$ is the unpolarized LO GRV [15] input gluon distribution. These two sets will be called ‘ $\Delta g = g$ input’ and ‘ $\Delta g = 0$ input’ scenarios, respectively. The gluon of set C of [10] is qualitatively different since it has a substantial negative polarization at large x . We will therefore also use this set in our calculations. For illustration, we show in Fig. 1 the gluon distributions of the four different sets of parton distributions we will use, taking a typical scale $Q^2 = 10 \text{ GeV}^2$. Keeping in mind that all four LO sets provide very good descriptions of the present polarized DIS data, it becomes obvious that the data indeed do not seem to be able to significantly constrain the x -shape of $\Delta g(x, Q^2)$.

In the case of photoproduction the electron just serves as a source of quasi-real photons which are radiated according to the Weizsäcker-Williams spectrum. The photons can then interact either directly or via their partonic structure (‘resolved’ contribution). In the case of longitudinally polarized electrons, the resulting photon will be longitudinally (more precisely, circularly) polarized and, in the resolved case, the *polarized* (helicity-weighted) parton distributions of the photon, $\Delta f^\gamma(x, Q^2)$, enter the calculations. Thus one can define the effective polarized parton densities at the scale M in the longitudinally polarized electron via¹

$$\Delta f^e(x_e, M^2) = \int_{x_e}^1 \frac{dy}{y} \Delta P_{\gamma/e}(y) \Delta f^\gamma(x_\gamma = \frac{x_e}{y}, M^2) \quad (1)$$

($f = q, g$) where $\Delta P_{\gamma/e}$ is the polarized Weizsäcker-Williams spectrum for which we will use

$$\Delta P_{\gamma/e}(y) = \frac{\alpha_{em}}{2\pi} \left[\frac{1 - (1-y)^2}{y} \right] \ln \frac{Q_{max}^2(1-y)}{m_e^2 y^2}, \quad (2)$$

with the electron mass m_e . For the time being, it seems most sensible to follow as closely as possible the analyses successfully performed in the unpolarized case, which implies to introduce the same kinematical cuts. As in [3, 5, 16] we will use an upper cut² $Q_{max}^2 = 4 \text{ GeV}^2$, and

¹We include here the additional definition $\Delta f^\gamma(x_\gamma, M^2) \equiv \delta(1-x_\gamma)$ for the direct (‘unresolved’) case.

²In H1 analyses of HERA photoproduction data [2, 4] the cut $Q_{max}^2 = 0.01 \text{ GeV}^2$ is used along with slightly different y -cuts as compared to the corresponding ZEUS measurements [3, 5], which leads to smaller rates.

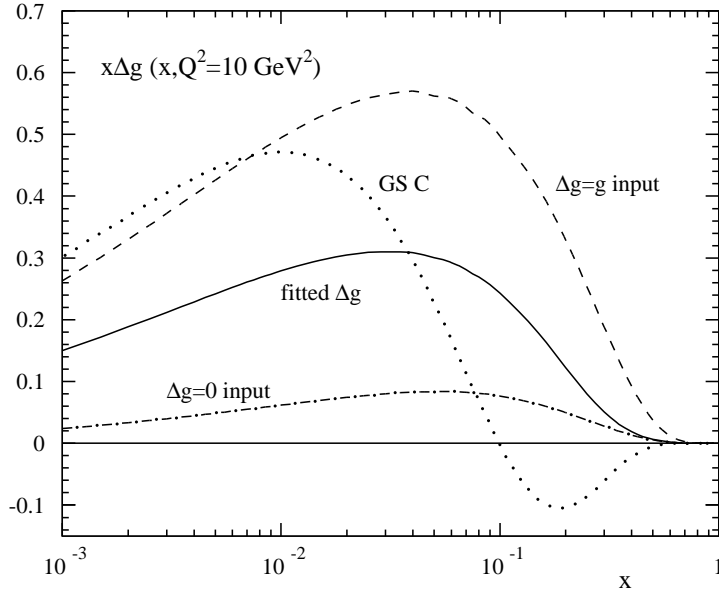


Figure 1: Gluon distributions at $Q^2 = 10 \text{ GeV}^2$ of the four LO sets of polarized parton distributions used in this paper. The dotted line refers to set C of [10], whereas the other distributions are taken from [9] as described in the text.

the y -cuts $0.2 \leq y \leq 0.85$ (for single-jet [3] production) and $0.2 \leq y \leq 0.8$ (for dijet [5] and single-inclusive hadron [6, 7] production) will be imposed.

The polarized photon structure functions $\Delta f^\gamma(x_\gamma, M^2)$ in (1) are completely unmeasured so far, so that models for them have to be invoked. To obtain a realistic estimate for the theoretical uncertainties in the polarized photonic parton densities two very different scenarios were considered in [17] assuming ‘maximal’ ($\Delta f^\gamma(x, \mu^2) = f^\gamma(x, \mu^2)$) or ‘minimal’ ($\Delta f^\gamma(x, \mu^2) = 0$) saturation of the fundamental positivity constraints $|\Delta f^\gamma(x, \mu^2)| \leq f^\gamma(x, \mu^2)$ at the input scale μ for the QCD evolution. Here μ and the unpolarized photon structure functions $f^\gamma(x, \mu^2)$ were adopted from the phenomenologically successful radiative parton model predictions in [18]. The results of these two extreme approaches are presented in Fig. 2 in terms of the photonic parton asymmetries $A_f^\gamma \equiv \Delta f^\gamma / f^\gamma$, evolved to $Q^2 = 30 \text{ GeV}^2$ in LO. An ideal aim of measurements in a polarized collider mode of HERA would of course be to determine the Δf^γ and to see which ansatz is more realistic. The sets presented in Fig. 2, which we will use in what follows, should in any case be sufficient to study the sensitivity of the various cross sections to the Δf^γ , but also to see in how far they influence a determination of Δg . We note that in [19] we have extended our studies of the polarized photon structure also to NLO.

We finally note that in what follows a polarized cross section will always be defined as

$$\Delta\sigma \equiv \frac{1}{2} \left[\sigma(++) - \sigma(+-) \right], \quad (3)$$

the signs denoting the helicities of the scattering particles. The corresponding unpolarized cross section is given by taking the sum instead, and the cross section asymmetry is $A \equiv \Delta\sigma/\sigma$. Whenever calculating an asymmetry A , we will use the LO GRV parton distributions for the proton [15] and the photon [18] to calculate the unpolarized cross section. For consistency, we will employ the LO expression for the strong coupling α_s with [9, 10, 17] $\Lambda_{QCD}^{(f=4)} = 200 \text{ MeV}$ for four active flavours.

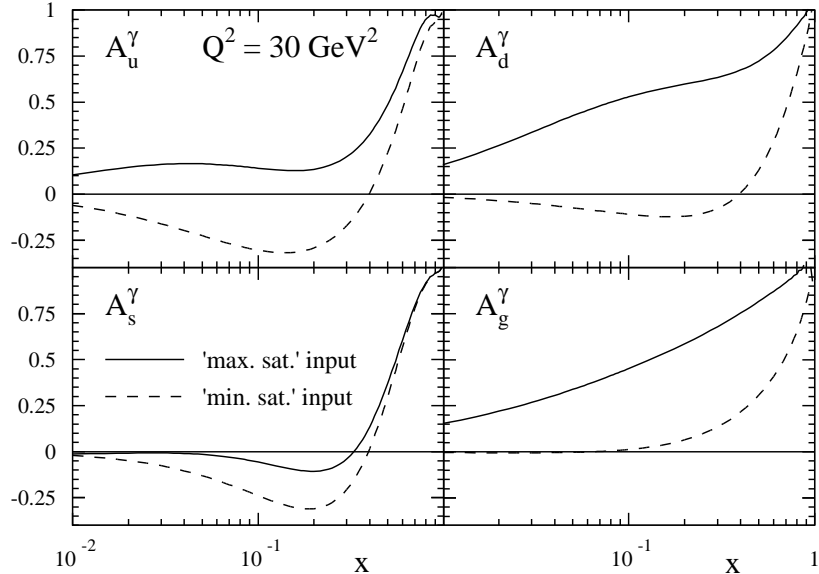


Figure 2: Photonic LO parton asymmetries $A_f^\gamma \equiv \Delta f^\gamma / f^\gamma$ at $Q^2 = 30 \text{ GeV}^2$ for the two scenarios considered in [17] (see text). The unpolarized LO photonic parton distributions were taken from [18].

3 Photoproduction Reactions at Polarized HERA

The generic LO cross section formula for the photoproduction of a single jet with transverse momentum p_T and cms-rapidity η in polarized ep collisions reads:

$$\frac{d^2 \Delta \sigma}{dp_T d\eta} = \sum_{f^e, f^p, c} \Delta f^e(x_e, M^2) \otimes \Delta f^p(x_p, M^2) \otimes \frac{d^2 \Delta \hat{\sigma}^{f^e f^p \rightarrow cd}}{dp_T d\eta}, \quad (4)$$

where \otimes denotes a convolution and the sum is running over all properly symmetrized $2 \rightarrow 2$ subprocesses for the direct ($\gamma b \rightarrow cd$, $\Delta f^e(x_e, M^2) \equiv \Delta P_{\gamma/e}(x_e)$) and resolved ($ab \rightarrow cd$) cases. When only light flavours are involved, the corresponding differential helicity-dependent LO subprocess cross sections can be found in [20]. In all following predictions we will deal with the charm contribution to the cross section by including charm only as a *final* state particle produced via the subprocesses $\gamma g \rightarrow c\bar{c}$ (for the direct part) and $gg \rightarrow c\bar{c}$, $q\bar{q} \rightarrow c\bar{c}$ (for the resolved part). For the values of p_T considered it turns out that the finite charm mass can be safely neglected in these subprocess cross sections. In (4), $\hat{s} \equiv x_e x_p s$ and M is the factorization/renormalization scale for which we will use³ $M = p_T$. The Δf^p stand for the polarized parton distributions of the proton. Needless to say that we obtain the corresponding unpolarized LO jet cross section $d^2 \sigma / dp_T d\eta$ by using LO unpolarized parton distributions and subprocess cross sections in (4).

It appears very promising [8] to study the η_{LAB} -distribution of the cross section and the asymmetry, where η_{LAB} is the laboratory frame rapidity, related to η via $\eta \equiv \eta_{cms} = \eta_{LAB} - \frac{1}{2} \ln(E_p/E_e)$. As usual, η_{LAB} is defined to be positive in the proton forward direction. The crucial point is that for negative η_{LAB} the main contributions are expected to come from the region $x_\gamma \rightarrow 1$ and thus mostly from the direct piece at $x_\gamma = 1$. To investigate this, Fig. 3 shows our results for the single-inclusive jet cross section and its asymmetry vs. η_{LAB} and integrated over $p_T > 8 \text{ GeV}$ for the four sets of the polarized proton's parton distributions. For Figs. 3a,b we

³The scale dependence of the theoretical LO predictions for the spin asymmetries – which are the quantities relevant in experiments – turns out to be rather weak, for a discussion see [8].

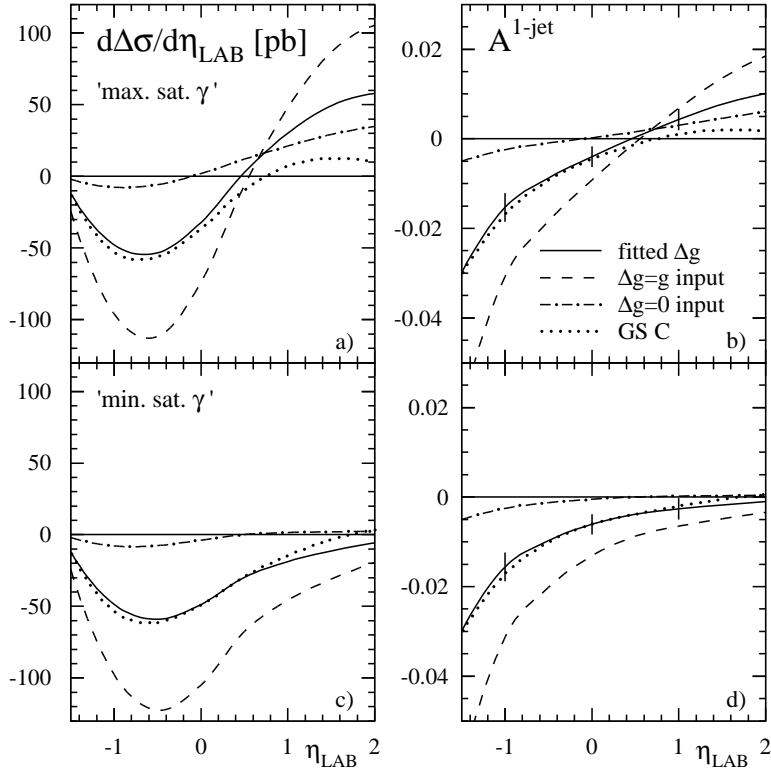


Figure 3: **a:** η_{LAB} -dependence of the polarized single-jet inclusive photoproduction cross section in ep -collisions at HERA, integrated over $p_T > 8$ GeV. The resolved contribution to the cross section has been calculated with the ‘maximally’ saturated set of polarized photonic parton distributions. **b:** Asymmetry corresponding to **a**. **c,d:** Same as **a,b**, but for the ‘minimally’ saturated set of polarized photonic parton distributions.

have used the ‘maximally’ saturated set of polarized photonic parton densities, whereas Figs. 3c,d correspond to the ‘minimally’ saturated one. Comparison of Figs. 3a,c or 3b,d shows that indeed the direct contribution clearly dominates for $\eta_{LAB} \leq -0.5$, where also differences between the polarized gluon distributions of the proton show up clearly. Furthermore, the cross sections are generally large in this region with asymmetries of a few percents. At positive η_{LAB} , we find that the cross section is dominated by the resolved contribution and is therefore sensitive to the parton content of both the polarized proton *and* the photon. This means that one can only learn something about the polarized photon structure functions if the polarized parton distributions of the proton are already known to some accuracy or if an experimental distinction between resolved and direct contributions can be achieved. We note that the dominant contributions to the resolved part at large η_{LAB} are driven by the polarized photonic *gluon* distribution Δg^γ . We have included in the asymmetry plots in Figs. 3b,d the expected statistical errors δA at HERA which can be estimated from

$$\delta A = \frac{1}{P_e P_p \sqrt{\mathcal{L} \sigma \epsilon}}, \quad (5)$$

where P_e, P_p are the beam polarizations, \mathcal{L} is the integrated luminosity and ϵ the jet detection efficiency, for which we assume $P_e * P_p = 0.5$, $\mathcal{L} = 100/\text{pb}$ and $\epsilon = 1$. From the results it appears that a measurement of the proton’s Δg should be possible from single-jet events at negative rapidities where the contamination from the resolved contribution is minimal.

In the unpolarized case, an experimental criterion for a distinction between direct and resolved contributions has been introduced [21] and used [5] in the case of dijet photoproduction at HERA. We will now adopt this criterion for the polarized case to see whether it would enable a further access to Δg and/or the polarized photon structure functions. The generic expression for the polarized cross section $d^3\Delta\sigma/dp_T d\eta_1 d\eta_2$ for the photoproduction of two jets with laboratory system rapidities η_1, η_2 has a form analogous to (4). Here one has

$$x_e \equiv \frac{p_T}{2E_e} (e^{-\eta_1} + e^{-\eta_2}) \quad , \quad x_p \equiv \frac{p_T}{2E_p} (e^{\eta_1} + e^{\eta_2}) \quad , \quad (6)$$

where p_T is the transverse momentum of one of the two jets (which balance each other in LO). Following [5], we will integrate over the cross section to obtain $d\Delta\sigma/d\bar{\eta}$, where $\bar{\eta} \equiv (\eta_1 + \eta_2)/2$. Furthermore, we will apply the cuts [5] $|\Delta\eta| \equiv |\eta_1 - \eta_2| \leq 0.5$, $p_T > 6$ GeV. The important point is that measurement of the jet rapidities allows for fully reconstructing the kinematics of the underlying hard subprocess and thus for determining the variable [5]

$$x_\gamma^{OBS} = \frac{\sum_{jets} p_T^{jet} e^{-\eta^{jet}}}{2yE_e} \quad , \quad (7)$$

which in LO equals $x_\gamma = x_e/y$ with y as before being the fraction of the electron's energy taken by the photon. Thus it becomes possible to experimentally select events at large x_γ , $x_\gamma > 0.75$ [21, 5], hereby isolating the *direct* contribution to the cross section with just a rather small contamination from resolved processes. Conversely, the events with $x_\gamma \leq 0.75$ will represent the resolved part of the cross section. This procedure should therefore be ideal to extract Δg on the one hand, and examine the polarized photon structure functions on the other.

Fig. 4 shows the results [8] for the direct part of the cross section according to the above selection criteria. The contributions from the resolved subprocesses have been included, using the ‘maximally’ saturated set of polarized photonic parton densities. They turn out to be non-negligible but, as expected, subdominant. More importantly, due to the constraint $x_\gamma > 0.75$ they are determined by the polarized quark, in particular the u -quark, distributions in the photon, which at large x_γ are equal to their unpolarized counterparts as a result of the Q^2 -evolution (see Fig. 2), rather *independently* of the hadronic input chosen. Thus the uncertainty coming from the polarized photon structure is minimal here and under control. As becomes obvious from Fig. 4, the cross sections are fairly large over the whole range of $\bar{\eta}$ displayed and very sensitive to the shape *and* the size of Δg with, unfortunately, not too sizeable asymmetries as compared to the statistical errors for $\mathcal{L} = 100/\text{pb}$. A measurement of Δg thus appears to be possible under the imposed conditions only if luminosities clearly exceeding $100/\text{pb}$ can be reached. Fig. 5 displays the same results, but now for the resolved contribution with $x_\gamma \leq 0.75$ for the ‘maximally’ saturated set (Figs. 5a,b) and the ‘minimally’ saturated one (Figs. 5c,d). As expected, the results depend on the parton content of both the polarized photon and the proton, which implies that again the latter has to be known to some accuracy to allow for the extraction of some information on the polarized photon structure. We emphasize that the experimental finding of a non-vanishing asymmetry here would establish at least the definite existence of a resolved contribution to the polarized cross section.

At a first glance, single-inclusive production of charged hadrons appears less interesting than jet production, as the cross section for producing a definite hadron at a given p_T will always be smaller than the one for a jet. On the other hand, in case of inclusive hadrons one can obviously go experimentally to p_T much smaller than the $p_T^{min} = 8$ GeV employed in our jet studies. Moreover, in the unpolarized case single-inclusive hadron production was successfully studied

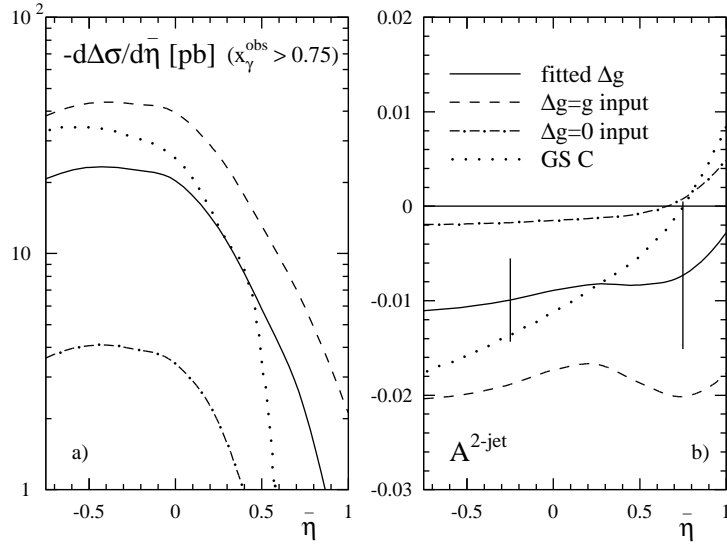


Figure 4: **a:** $\bar{\eta}$ -dependence of the 'direct' part ($x_\gamma^{OBS} > 0.75$) of the polarized two-jet photoproduction cross section in ep -collisions at HERA for the four different sets of polarized parton distributions of the proton. **b:** Asymmetry corresponding to **a**. The expected statistical errors indicated by the bars have been calculated according to (5) and as explained in the text.

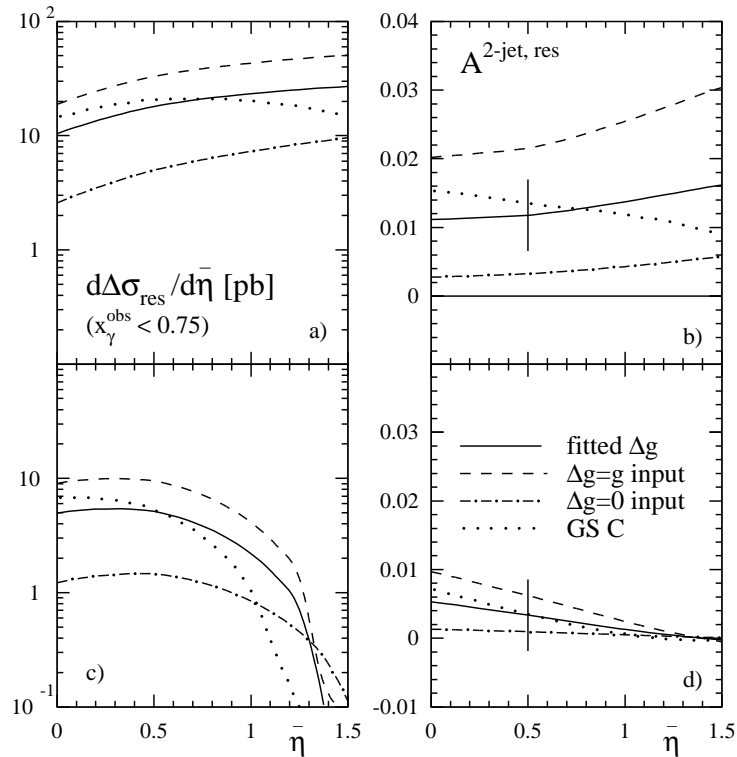


Figure 5: Same as Fig. 4, but for the resolved part of the cross section, defined by $x_\gamma^{OBS} \leq 0.75$ (see text). For **a,b** the 'maximally' saturated set of polarized photonic parton distributions has been used and for **c,d** the 'minimally' saturated one.

experimentally at HERA prior to jets [6, 7]. The expression for the cross section for single-inclusive hadron production is similar to the one in (4), but comprises an additional convolution with the function D_c^h describing the fragmentation of particle c into the hadron h . For the D_c^h we will use the LO fragmentation functions of [22] which yield a good description of the unpolarized HERA inclusive hadron data [6, 7]. Figs. 6a,b show our results for the sum of charged pions and kaons after integration over $p_T > 3$ GeV, where all other parameters were chosen exactly as for Figs. 3a,b (since the sensitivity of the results to the polarized photon structure is qualitatively similar to the one-jet case we only consider the ‘maximally’ saturated photon scenario here). One can see that the cross sections and their asymmetries behave similarly in shape as the corresponding results in Figs. 3a,b, but are somewhat smaller in magnitude. Nevertheless, the expected statistical errors, calculated for the rather conservative choices $P_e * P_p = 0.5$, $\mathcal{L} = 100/\text{pb}$ and $\epsilon = 0.8$ in Eq. (5) and displayed in Fig. 6b, demonstrate that single-inclusive hadron photoproduction remains a promising candidate.

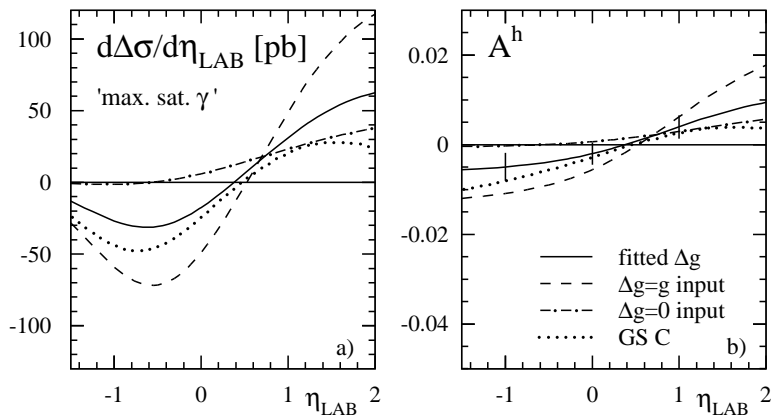


Figure 6: **a,b:** Same as Figs. 3a,b, but for the case of single-inclusive charged hadron production, integrated over $p_T > 3$ GeV.

4 NLO Corrections to Polarized Single-Inclusive Hadron Photoproduction

One major uncertainty concerning our LO results presented in the previous section is expected to reside in the NLO corrections and the extent by which they affect the cross sections and spin asymmetries relevant for experimental measurements. Only when the corrections are reasonably small and under control can a process that shows good sensitivity to, say, Δg at the lowest order, be regarded as a genuine probe of the polarized gluon distribution and be reliably used to extract it from future data. The first basic ingredient for an extension of our results to NLO has been provided in the past two years by the fact mentioned above that NLO fits to polarized DIS data have been performed, yielding spin-dependent nucleon parton distributions evolved to NLO accuracy. Focusing on the direct part of single-inclusive hadron photoproduction, the calculation of the polarized cross section to NLO is then completed by using also (unpolarized) NLO fragmentation functions for the produced hadron (as provided in [22]), and by including the $\mathcal{O}(\alpha_s)$ corrections to the spin-dependent direct subprocess cross sections for the inclusive production of a certain parton that fragments into the hadron. The latter corrections have been obtained very recently [14]. Technically, they involve calculation of the virtual corrections to

the Born graphs $\vec{\gamma}\vec{q} \rightarrow gq$, $\vec{\gamma}g \rightarrow q\bar{q}$ and of the $2 \rightarrow 3$ contributions $\vec{\gamma}\vec{a} \rightarrow bcd$, a, b, c, d being arbitrary partons and the arrows denoting longitudinal polarization.

We emphasize that the direct part of its own is no longer a well-defined quantity beyond LO since it depends on the factorization scheme adopted. This fact is well-known from the unpolarized case, in which the corrections to the direct [23] and to the resolved [24] contributions have all been calculated. Therefore our results reported here will only be the first step in a full calculation of NLO effects to polarized single-inclusive hadron photoproduction. Despite the fact that they are not complete in this sense, we believe our results to be very important both phenomenologically and theoretically: As mentioned earlier, the direct component dominates for HERA kinematics at $\eta_{LAB} \leq -0.5$. Our NLO corrections for the direct part should also already be sufficient to shed some light on the general question of perturbative stability of the process considered.

Fig. 7 displays the K -factors for the direct part of the polarized cross section for single-inclusive hadron photoproduction, where

$$K \equiv d\Delta\sigma^{NLO}/d\Delta\sigma^{LO} . \quad (8)$$

The LO direct cross section has been calculated as in the previous figures. For the (scheme-dependent) NLO one we have chosen the $\overline{\text{MS}}$ scheme and used also NLO ($\overline{\text{MS}}$) fragmentation functions [22] and spin-dependent parton distributions [9], as well as the two-loop expression for α_s . As can be seen from Fig. 7, the K -factors are close to unity, implying that the NLO corrections are rather mild. For comparison, we also show the K -factor for the unpolarized cross section. Since both the direct [23] and the resolved [24] contributions can be consistently calculated to NLO in this case, we are able to plot the full physical (scheme-independent) result.

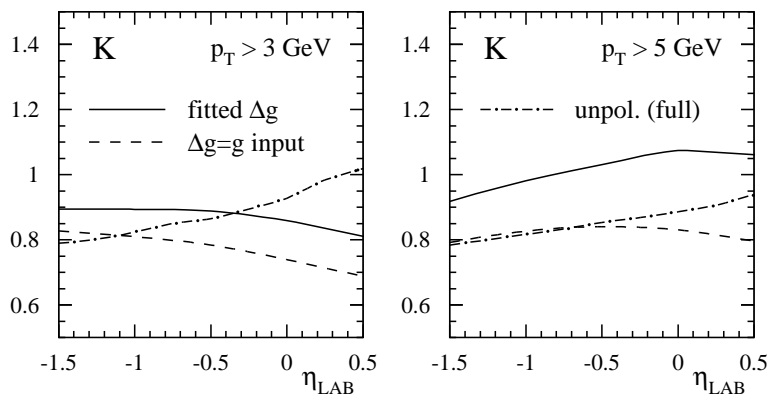


Figure 7: K -factors for the direct part of the polarized single-inclusive hadron photoproduction cross section. Also shown is the K -factor for the full ('direct + resolved') unpolarized cross section.

5 Conclusions

We have analyzed various photoproduction experiments in the context of a polarized ep -collider mode of HERA. We have found very encouraging results for jet and single-inclusive hadron production which look promising tools for a determination of the polarized gluon distribution of the proton and, possibly, might even allow access to the completely unknown parton content of a polarized photon. We have also presented for the first time the NLO corrections to the direct part of the polarized single-inclusive hadron photoproduction cross section, which reveal good

perturbative stability. The proposed measurements will not be easy to do, but they seem a very interesting challenge for the future at HERA.

Acknowledgements: I am grateful to D. de Florian and M. Stratmann for a fruitful and pleasant collaboration.

References

- [1] For an overview see J. Feltesse and A. Schäfer, in: Proc. of the 1995/96 workshop on ‘Future Physics at HERA’, eds. G. Ingelman et al., p.760.
- [2] I. Abt et al., H1 collab., *Phys. Lett.* **B314** (1993) 436.
- [3] M. Derrick et al., ZEUS collab., *Phys. Lett.* **B342** (1995) 417.
- [4] T. Ahmed et al., H1 collab., *Nucl. Phys.* **B445** (1995) 195.
- [5] M. Derrick et al., ZEUS collab., *Phys. Lett.* **B348** (1995) 665.
- [6] I. Abt et al., H1 collab., *Phys. Lett.* **B328** (1994) 176.
- [7] M. Derrick et al., ZEUS collab., *Z. Phys.* **C67** (1995) 227.
- [8] M. Stratmann and W. Vogelsang, *Z. Phys.* **C74** (1997) 641; Proc. of the 1995/96 workshop on ‘Future Physics at HERA’, eds. G. Ingelman et al., p.815.
- [9] M. Glück, E. Reya, M. Stratmann and W. Vogelsang, *Phys. Rev.* **D53** (1996) 4775; M. Stratmann, these proceedings.
- [10] T. Gehrmann and W.J. Stirling, *Phys. Rev.* **D53**, (1996) 6100.
- [11] D. de Florian and R. Sassot, CERN-TH/97-71; D. de Florian, these proceedings.
- [12] E. Leader, A.V. Sidorov and D.B. Stamenov, [hep-ph/9708335](#).
- [13] R.D. Ball, S. Forte and G. Ridolfi, *Phys. Lett.* **B378** (1996) 255; G. Altarelli, R.D. Ball, S. Forte and G. Ridolfi, *Nucl. Phys.* **B496** (1997) 337.
- [14] D. de Florian and W. Vogelsang, CERN-TH/97-280; D. de Florian, these proceedings.
- [15] M. Glück, E. Reya and A. Vogt, *Z. Phys.* **C67** (1995) 433.
- [16] M. Klasen, G. Kramer and S.G. Salesch, *Z. Phys.* **C68** (1995) 113; M. Klasen and G. Kramer, *Phys. Lett.* **B366** (1996) 385; *Z. Phys.* **C72** (1996) 107.
- [17] M. Glück and W. Vogelsang, *Z. Phys.* **C55** (1992) 353; **C57** (1993) 309; M. Glück, M. Stratmann and W. Vogelsang, *Phys. Lett.* **B337** (1994) 373.
- [18] M. Glück, E. Reya and A. Vogt, *Phys. Rev.* **D46** (1992) 1973.
- [19] M. Stratmann and W. Vogelsang, *Phys. Lett.* **B386** (1996) 370.
- [20] J. Babcock, E. Monsay and D. Sivers, *Phys. Rev.* **D19** (1979) 1483.
- [21] J.R. Forshaw and R.G. Roberts, *Phys. Lett.* **B319**, (1993) 539.
- [22] J. Binnewies, B.A. Kniehl and G. Kramer, *Phys. Rev.* **D52** (1995) 4947.
- [23] P. Aurenche, A. Douiri, R. Baier, M. Fontannaz and D. Schiff, *Phys. Lett.* **135B** (1984) 164; *Nucl. Phys.* **B286** (1987) 553; L.E. Gordon, *Phys. Rev.* **D50** (1994) 6753.
- [24] F. Aversa, P. Chiappetta, M. Greco and J.Ph. Guillet, *Phys. Lett.* **B210** (1988) 225; **B211** (1988) 465; *Nucl. Phys.* **B327** (1989) 105.